Astroparticle Physics 83 (2016) 1–5

Contents lists available at ScienceDirect

Astroparticle Physics

journal homepage: www.elsevier.com/locate/astropartphys

The small contribution of molecular Bremsstrahlung radiation to the air-fluorescence yield of cosmic ray shower particles

Imen Al Samarai[a], Olivier Deligny[b,*], Jaime Rosado[c]

[a] Laboratoire de Physique Nucléaire et des Hautes Énergies, CNRS/IN2P3 & Universités Pierre et Marie Curie and Paris Diderot, Paris Cedex 75252, France
[b] Institut de Physique Nucléaire, CNRS-IN2P3, Univ. Paris-Sud, Université Paris-Saclay, Orsay Cedex 91406, France
[c] Departamento de Física Atómica, Molecular y Nuclear, Facultad de Ciencias Físicas, Universidad Complutense de Madrid, Madrid E-28040, Spain

ARTICLE INFO

Article history:
Received 16 March 2016
Revised 9 June 2016
Accepted 13 June 2016
Available online 16 June 2016

Keywords:
extensive air showers
fluorescence yield
molecular bremsstrahlung radiation

ABSTRACT

A small contribution of molecular Bremsstrahlung radiation to the air-fluorescence yield in the UV range is estimated based on an approach previously developed in the framework of the radio-detection of showers in the gigahertz frequency range. First, this approach is shown to provide an estimate of the main contribution of the fluorescence yield due to the de-excitation of the C $^3\Pi_u$ electronic level of nitrogen molecules to the B $^3\Pi_g$ one amounting to $Y_{[337]} = (6.05 \pm 1.50)$ MeV^{-1} at 800 hPa pressure and 293 K temperature conditions, which compares well to previous dedicated works and to experimental results. Then, under the same pressure and temperature conditions, the fluorescence yield induced by molecular Bremsstrahlung radiation is found to be $Y^{\rm MBR}_{[330-400]} = 0.10$ MeV^{-1} in the wavelength range of interest for the air-fluorescence detectors used to detect extensive air showers induced in the atmosphere by ultra-high energy cosmic rays. This means that out of ≃175 photons with wavelength between 330 and 400 nm detected by fluorescence detectors, one of them has been produced by molecular Bremsstrahlung radiation. Although small, this contribution is not negligible in regards to the total budget of systematic uncertainties when considering the absolute energy scale of fluorescence detectors.

1. Introduction

Ultra-high energy cosmic rays can be efficiently observed by collecting the isotropic atmospheric fluorescence light emitted during dark nights by the extensive air showers that they induce. This detection technique, pioneered by the Fly's Eye experiment [1], was used by the HiRes experiment [2] and is currently used at the Pierre Auger Observatory [3] and the Telescope Array [4]. Fluorescence telescopes allow an accurate observation of the longitudinal profile of the showers. Based on the assumption that the fluorescence intensity is proportional to the electromagnetic energy deposited by the shower in the atmosphere, the fluorescence detection technique provides the opportunity of performing shower calorimetry by mapping the ionisation content along the shower tracks. It is, as of today, the most direct way to measure the primary energy on a nearly model-independent basis.

The various processes leading to the air-fluorescence emission have been well investigated theoretically in the recent years [5–7]. The atmospheric fluorescence produced in an extensive air shower is now known to be due mainly to the de-excitation of nitrogen molecules previously excited by the numerous low-energy ionisation electrons left in the atmosphere after the passage of the electrons/positrons of the shower front. Low-energy ionisation electrons can in turn produce their own emission through the molecular Bremsstrahlung process, as a consequence of their collisions with nitrogen or oxygen targets. The corresponding radiation is expected to occur over a wide range of frequencies; and the purpose of this work is to quantify the contribution of the molecular Bremsstrahlung radiation to the air-fluorescence light emitted in the UV wavelength range.

The general approach follows from previous works dedicated to the emission in the gigahertz frequency range [8,9], applied here to the UV wavelength range. To start with, a comprehensive treatment of the time evolution of the distribution function describing the low-energy ionisation electrons produced after the passage of high-energy electrons in air is presented in Section 2. From the knowledge of this distribution function, the fluorescence yield expected from the de-excitation of nitrogen molecules is estimated in Section 3 and is shown to compare favorably to the various measurements under 800 hPa pressure and 293 K temperature conditions. Then, with the same pressure and temperature conditions, the application of the formalism to the fluorescence yield expected

* Corresponding author.
E-mail addresses: ialsamar@lpnhe.in2p3.fr (I. Al Samarai), deligny@ipno.in2p3.fr (O. Deligny), jaime_ros@fis.ucm.es (J. Rosado).

http://dx.doi.org/10.1016/j.astropartphys.2016.06.006
0927-6505/

from molecular Bremsstrahlung radiation is presented in Section 4. Finally, conclusions are given in Section 5.

2. Production and interactions of low-energy ionisation electrons

Throughout this study, the case of primary electrons with typical energy of a few tens of mega-electron volts is considered. Upon the passage of such high-energy electrons in air, there is roughly 2 MeV g^{-1} cm^2 of deposited energy per grammage unit mainly through the ionisation process. Hence, for one primary electron with energy T_p propagating over an infinitesimal distance dx in air, and for a mass density and average molar mass of dry air of target molecules ρ and A, the average number of ionisation electrons per unit length and per kinetic energy band can be estimated as

$$\frac{d^2 n_{e,i}(T_p, T)}{dx\, dT} = \frac{\rho \mathcal{N}}{A} \sigma_{ion}(T_p) f_0(T_p, T), \tag{1}$$

with $\mathcal{N}$ the Avogadro number. The ionisation cross section $\sigma_{ion}(T_p)$ is considered identical for nitrogen or oxygen targets in this study. $f_0(T)$ stands for the normalised distribution in kinetic energy of the ionisation electrons at their time of creation, $f_0(T) \equiv f(T, t = 0)$. This distribution has been experimentally determined and accurately parameterised for primary high-energy electrons with kinetic energies up to several kilo-electron volts [10]. For higher kinetic energies T_p, relativistic effects as well as close collisions giving rise to the emission of fast secondary electrons (knock-on electrons) are known to modify the f distribution. To account for these effects, we adopt the analytical expression provided in [6]:

$$f_0(T_p, T) = \frac{8\pi Z R_y^2}{m(\beta(T_p)c)^2} \frac{1 + C \exp(-T/T_k)}{T^2 + \overline{T}^2}, \tag{2}$$

where c is the speed of light, m is the electron mass, β is the relativistic factor, R_y is the Rydberg constant, T ranges from 0 to $T_{max} = (T_p - I_0)/2$ due to the indistinguishability between primary and secondary electrons (with I_0 the ionisation potential to create an electron–ion pair in air), the constant C is determined in the same way as in [10] so that $\int dT\, f_0(T)$ reproduces the total ionisation cross section, $T_k = 77$ eV is a parameter acting as the boundary between close and distant collisions, and $\overline{T} = 11.4\,(15.2)$ eV for nitrogen (oxygen) [11]. In the energy range of interest, this expression leads to $\langle T \rangle \simeq 40$ eV, in agreement with the well-known stopping power. It should be noted, however, that the above equation does not include all the relativistic and exchange effects in the energy distribution of ionisation electrons [7], but these effects are unimportant for a primary kinetic energy of 60 MeV assumed in this work.

The quantity given by Eq. (1) corresponds to the average number of secondary electrons per length and per kinetic energy unit left just after the passage of one primary high-energy electron in air. The same quantity available at any time t after the passage of one primary high-energy electron is governed by the interactions that these electrons undergo in air. In turn, the evolution in time of the left hand side of Eq. (1) can be fully encompassed in the time dependence of the distribution in kinetic energy $f(T, t)$ of the ionisation electrons (note that, for convenience, we drop hereafter the T_p dependence). This evolution is determined by a Boltzmann equation accounting for all the interactions of interest at work. Considering the ionisation as quasi-static in space given the low energy of the electrons, it can be shown that the dominant term governing the time evolution of f is the collision one [9]:

$$\frac{\partial f(T,t)}{\partial t} = \frac{\mathcal{N}c}{A}\Bigg[- \sum_{m=N_2,O_2} \rho_m \beta(T) \left(\sigma^m_{ion}(T) + \sigma^m_{exc}(T)\right) f(T,t)$$

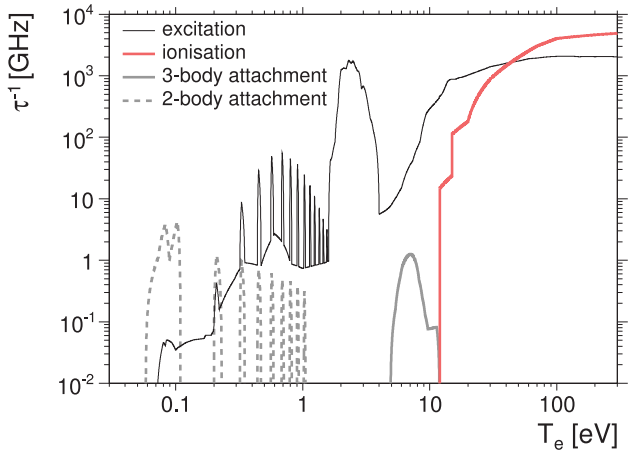

Fig. 1. Dominant collision rates for low-energy electrons in air, at sea level for a water concentration of 3000 ppm.

$$- \sum_{m=CO_2,H_2O} \rho_m \beta(T) \sigma^m_{exc}(T) f(T,t) - \rho_{O_2} \beta(T) \sigma^{O_2}_{att}(T) f(T,t)$$
$$+ \sum_{m=N_2,O_2} \rho_m \int_T^{T^{max}} dT' \beta(T')$$
$$\times \left(\frac{d\sigma^m_{ion}}{dT}(T', T) + \frac{d\sigma^m_{ion}}{dT}(T', T' - T - I_0) \right) f(T', t)$$
$$+ \sum_{m=N_2,O_2,CO_2,H_2O} \rho_m \int_T^{T^{max}} dT' \beta(T') \frac{d\sigma^m_{exc}}{dT}(T', T) f(T', t) \Bigg], \tag{3}$$

where σ^m_i denotes the cross sections of interest, namely ionisation, excitation of electronic levels (including ro-vibrational excitation) and attachment processes for a molecule m. The three first terms in the right hand side stand for the disappearance of electrons with kinetic energy T, while the two last terms stand for the appearance of electrons with kinetic energy T due to ionisation and excitation reactions initiated by electrons with higher kinetic energy T'. Note that in the case of ionisation, a second electron emerges from the collision with kinetic energy $T' - T - I_0$.

All cross sections of interest for this study are taken from experimental tabulated data in [12] and are shown in Fig. 1 as a function of the kinetic energy. For completeness, rates are shown down to kinetic energies much lower than those relevant for the production of UV photons. Going down in energy, the main features of the different rates can be summarised in the following way:

- For $T \geq 40$ eV, ionisation on N_2 and O_2 molecules is the dominant process, causing energy losses on a time scale below a picosecond.
- For 4 eV $\leq T \leq$ 40 eV, excitation on electronic levels of N_2 and O_2 molecules is the dominant process. The corresponding energy losses occur on time scales going from picoseconds to a few nanoseconds when going down in energy. To a smaller extent, there is a disappearance of electrons through the three-body attachment process.
- For 1.7 eV $\leq T \leq$ 4 eV, resonances for excitation on N_2 and O_2 molecules through ro-vibrational processes cause energy losses on a time scale of the picosecond.
- For 0.2 eV $\leq T \leq$ 1.7 eV:
  - Resonances for excitation on N_2 and O_2 molecules through ro-vibrational processes quantised in energies are visible through the peaks in continuous line. The corresponding energy losses occur on a time scale of a few tens of picoseconds.